Monitoring of a Concentrating Solar Thermal Field: Energy Measurements and Uncertainty Analysis

Marco Cozzini, Mauro Pipiciello, Roberto Fedrizzi
Institute for Renewable Energy
EURAC Research
Viale Druso 1, I-39100 Bolzano, Italy

Abstract—**This paper deals with the monitoring of a solar thermal field setup with concentrating linear Fresnel collectors. This work describes types of sensors installed in the field and energy performance measurements, presenting a detailed analysis about uncertainty propagation. The results are critically discussed taking into account the different perspectives of detailed performance assessment and the industrial needs of real installations.**

Keywords—Solar thermal energy, solar process heat, linear Fresnel collectors, uncertainty analysis

I. INTRODUCTION

In the field of renewable energies it is important to carry out detailed monitoring campaigns, as there is still significant technological development in progress. Moreover, even in the presence of mature technologies, it is important to assess their performance in applications not tested before, due to the intermittent nature of renewable sources, which makes more difficult to extrapolate the results of laboratory tests.

Within the European FP7 project InSun, the application of solar heat to industrial process is studied through demonstration activities. In principle, solar process heat exhibits a high potential, due to the large number of manufacturing activities requiring heat in the low-medium temperature range [1], [2]. Among the activities of the InSun project, the testing of newly developed linear Fresnel collectors (LFCs) – with promising features for the reduction of capital
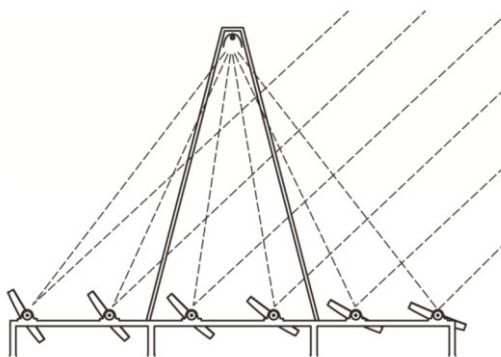

Fig. 1. Section drawing of a linear Fresnel collector (courtesy of Soltigua). Dashed lines represent sun rays, reflected first by the mirrors constituting the primary optics and then by a small secondary optics located above the receiver tube.

costs – has been implemented. The collectors (developed by Soltigua, a partner of the InSun project) can cover a medium temperature range, approximately up to 250 °C. Within the project they have been installed in Gambettola (Italy) and have been applied to the generation of hot air used for the drying process of a brick manufacturing [3].

LFCs are a technology similar to the better-known concentrating parabolic trough collectors (PTCs). With respect to PTCs, LFCs substitute the large parabolic mirror with a set of smaller mirrors aligned on the horizontal plane (Fig. 1), with a concept similar to that of Fresnel lenses. This allows to reduce mirror curvature, giving rise to lower manufacturing costs and additional benefits, as lower wind loads. On the other hand, splitting the primary optics into several components typically reduces the optical efficiency.

These aspects, and in particular the differences between PTCs and LFCs have been discussed in a few papers [4], [5], [6], but in general Fresnel collectors can be considered a rather young technology with a rather limited literature [7], [8]. This makes important collecting additional data on these systems, especially with respect to real field operation. The dynamic testing of concentrating collectors is however a topic still under evolution. Until few years ago, the standard EN 12975:2006 [9] – developed for flat plate collectors, but including distinctions between direct and diffuse radiation and providing quasi-dynamic performance test specifications – was occasionally applied also to concentrating collectors [10]. Under the impulse of the European project QAiST (Quality Assurance in Solar heating and cooling Technology) and of the SHC programme of the International Energy Agency (Task 43), a joint collaboration between the European Committee for Standardization (CEN) and the International Organization for Standardization (ISO) was started, as described in [11]. In 2013, this yielded the new standard EN ISO 9806:2013 [12]. The latter applies to both flat plate and concentrating collectors, generalizing the content of EN 12975 with some refinements. However, according to [13], the new standard still misses to properly address all the issues related to the testing of concentrating collectors with variable geometry, thereby including linear Fresnel collectors.

The above standards clearly consider rather controlled test conditions, as necessary to limit the experiments in time and space and make them feasible in an "outdoor-laboratory" environment. Actually, transient effects are partially taken into

account with the so-called quasi-dynamic conditions. This is indeed crucial for solar systems, where truly stationary conditions are never reached. However, in the tests prescribed by standards, operating parameters like flow rate and temperatures are always kept within limited boundaries, so that significant measurement issues are avoided. The situation can be quite different in field measurements, as those considered in this paper. In this case, operating conditions can vary significantly, even under clear sky conditions. For example, the initial heating phase of the plant implies a transient which significantly affects the overall performance. Assessing the measurement uncertainties in such a situation, where the operating parameters can easily vary by a factor of three, is therefore a fundamental requisite.

In this context, this paper aims at clarifying aspects typically overlooked in thermal energy monitoring. We present the sensor choices done for this application and emphasize the varying value of the uncertainties under different operating conditions, discussing the issues related to their propagation to thermal energy metering. Although apparently academic, this analysis strongly relates to the degree of confidence solar collectors' manufacturers can hold when selling the energy performance of their product.

II. SOLAR FIELD LAYOUT

The LFC solar field studied here heats a hot thermal fluid (HTF) given by diathermic oil (Therminol SP). The field consists of four parallel loops of collectors, each loop containing two collector blocks of about 36 m each, for a total aperture of 1048 m^2. The solar energy is used to heat the diathermic oil up to about 250 °C. The absorbed heat is then transferred to a steam generator. The steam produced heats the air used in the mentioned brick drying process.

Thermal energy is measured from temperature and flow sensors located as in Fig. 2. The choice of the sensors done by Soltigua aimed to a compromise between monitoring accuracy and costs, trying to identify an acquisition system replicable in commercial installations.

For each of the four loops one can recognize the presence of three temperature sensors (e.g., for the bottom left loop, sensors T_{HTF1}, T_{HTF2}, T_{HTF3}) and one flow rate sensor (e.g., for the same loop, M_{HTF1}). Besides sensors monitoring single loops, similar sensors for the monitoring of the entire field are present ($T_{HTF,IN}$, $T_{HTF,OUT}$, M_{HTF}). Finally, sensors for the measurement of the direct normal irradiance (DNI) and of the ambient temperature are present (respectively denoted as R_{direct} and T_{amb} in the figure). The field also includes a three-way valve to bypass the heat exchanger during the pre-heating phase.

The described sensors' system allows for the measurement of the performance of different parts of the field. In this way, the operation of single loops and even of single collectors can be monitored. Apart from assessing the correct operation of single components, a rather detailed thermal efficiency measurement can be attempted in some cases. This is particularly important, as the nominal efficiencies assessed in laboratory conditions are not always well representative for on-field applications: indeed, while laboratory tests are typically
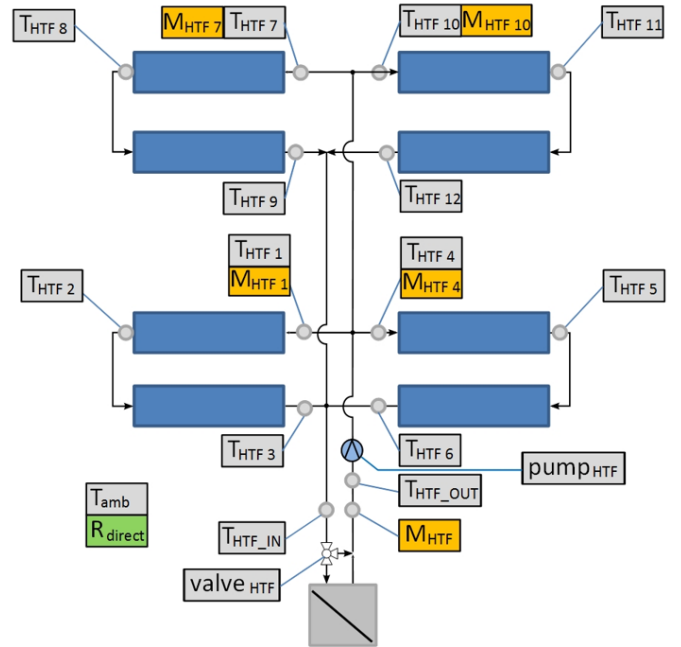

Fig. 2. Layout of the HTF field, running diathermic oil.

carried out in stationary conditions, the real operation of a solar field can be strongly affected by dynamic effects related to transient conditions (e.g., during the initial pre-heating phase).

III. UNCERTAINTY ANALYSIS

The present section focuses on the analysis of measurement uncertainty. First, an overview of the installed sensor types is presented. Then, uncertainty propagation for power and energy measurements is discussed.

A. Sensor types

In order to measure the thermal energy carried by diathermic oil, temperature and flow measurements are needed. The monitoring of the ambient temperature is also useful to interpret thermal losses, while clearly the measurement of the solar irradiance is crucial to assess the plant performance.

1) Temperature sensors

The chosen temperature sensors are Pt100 class B sensors. The uncertainty is $(0.3 + 0.005 \times |T|)$ °C (where T is the temperature measured in Celsius degrees). It is clear that the uncertainty significantly depends on temperature, especially at the operating conditions expected for diathermic oil. Note that with respect to these uncertainty values, the uncertainty deriving from the electronics is negligible. For more accurate temperature sensors, it could instead be necessary to consider the entire acquisition chain.

Energy measurements in fluids involve measures of temperature differences (see below), so that the resulting relative uncertainties can be large in some cases. On the other hand, it is worth pointing out that the nature of error in these sensors is mainly of systematic type, so that the composite uncertainty for differential measurements could be lower than what expected for purely uncorrelated measurements.

2) Flow rate sensors

Flow rate is measured through orifice plates. This type of measurement is based on a differential pressure measurement at the opposite sides of the orifice, with properly designed connections. Several details must be taken into account to convert the differential pressure measurement in an accurate mass flow measurement. This will be explained in the uncertainty propagation section. Here, we only discuss the uncertainty of the differential pressure sensors, available in two sizes (one for the pipes within collector loops, one for the main pipes). For both sensors, the uncertainty is 0.25 % of full scale (f.s.), full scale being 140 mbar for the sensor at main pipes and 110 mbar for the sensors at collector loops. However, a permanent bias of the order of 0.5-1 mbar was observed in all sensors (even in the absence of flow). Zero offset compensation was performed for some tests, but after each operation cycle (e.g., one day) the offset appeared again. According to the supplier, this behavior could be due to the trapping of air bubbles in the thin connection pipes, an effect potentially arising under operation. As the corresponding offset is not constant in time, it was treated as an additional source of uncertainty. It was hence deemed appropriate to assume an overall relative uncertainty of about 1 % for these sensors (typical operating conditions: 22-90 mbar for the sensor at main pipes, 15-60 mbar for the sensors at collector loops).

3) Solar irradiance sensor

Two solutions have been tested in the installed field, namely a solution based on a pyranometer (typically used for global irradiance) and a solution based on a pyrheliometer (specifically designed for the measurement of direct normal irradiance). For the pyranometer (first class ISO 9060), a custom-made casing was realized, in order to convert it into a low-cost sensor for the measurement of DNI (once installed on a proper tracking system). The installation of the highly accurate pyrheliometer (relative uncertainty of about 2 %) allowed to assess the relative uncertainty of the former sensor at the order of 9 %.

B. Uncertainty propagation in thermal power and energy measurements

In this section we discuss the uncertainty propagation for thermal power and energy.

1) Thermal power

Thermal power P_{th} in a flowing fluid can be estimated as the enthalpy difference between inlet and outlet. In terms of the mass flow rate Q_m and of the specific enthalpy h one simply has $P_{th} = Q_m (h_{out} - h_{in})$. From the point of view of uncertainty propagation, it is convenient to approximate the specific enthalpy in terms of specific heat C_p, according to

$$h_{out} - h_{int} = \int C_p(T)\, dT = C_p(<T>) \Delta T + O(\Delta T^3), \qquad (1)$$

where the integral is taken between the inlet and the outlet temperatures T_{in} and T_{out}, $<T> = (T_{in} + T_{out})/2$ is the corresponding average fluid temperature, while the temperature difference is given by $\Delta T = (T_{out} - T_{in})$. For the specific heat of diathermic oil we used the data sheet provided by the manufacturer, see appendix.

Neglecting the third order term in (2), one then gets

$$P_{th} = Q_m C_p(<T>) \Delta T, \qquad (2)$$

showing that the two main sources of uncertainty in thermal power measurements are mass flow rate and temperature difference (see appendix for the uncertainty of specific heat). They are discussed in detail in the following paragraphs.

For a product, the relative uncertainty is easily calculated from the relative uncertainties of the factors:

$$\sigma_{Pth} / P_{th} = \sqrt{[(\sigma_{Qm} / Q_m)^2 + (\sigma_{\Delta T} / \Delta T)^2]}, \qquad (3)$$

where we neglected the specific heat uncertainty and assumed uncorrelated quantities.

Mass flow rate. Mass flow rate measurements can be carried out with different technologies. As mentioned above, the choice adopted here relies on the differential pressure measured at the ends of an orifice plate. This is a cost effective and widely used solution, but it involves some non-trivial details, as follows.

As any liquid, oil can be considered incompressible, so that, with a good approximation, in turbulent regime the pressure drop Δp turns out to be proportional to Q_m^2/ρ, where ρ is the fluid density (significantly dependent on temperature for oil) and the proportionality factor mainly depends on the orifice geometry. For the orifices with the smallest size (collector loops), the standard ASME MFC 14M [14] can be used for a more accurate relation, while for the larger orifice (main pipes) the standard ISO 5167-2:2003 [15] can be used. However, the complicated relations $\Delta p(Q_m)$ contained in these standards cannot be inverted analytically to get the flow rate as a function of the pressure drop, so that they are impractical for uncertainty propagation. On the other hand, the correction terms with respect to the simple incompressible relation mentioned above are small, so that they can be mostly neglected when calculating uncertainty. One indeed has

$$Q_m = k_0 (1 + \varepsilon) \sqrt{(\rho \Delta p)}, \qquad (4)$$

where the coefficient k_0 only depends on geometrical parameters and the correction ε, while depending on the Reynolds number (and hence on the fluid operating conditions), is negligible for uncertainty propagation as $\varepsilon << 1$. The uncertainty of mass flow rate thereby derives from three main sources:

- Geometric uncertainty of the orifice plate. According to the supplier, this is in the range 0.7-0.8 % (relative) depending on the orifice size.

- Uncertainty of oil density $\rho(T)$, here in the range of 0.05-0.15 % (relative; see appendix).

- Uncertainty of differential pressure, here of the order of 1 % (relative), as mentioned above.

In conclusion, when using formulas taken from standards to evaluate the mass flow rate, the corresponding propagated relative uncertainty in nominal conditions is about 1 %. Note that these calculations are valid for the turbulent regime, above Reynolds numbers larger than about 4000-5000.

Temperature difference. The uncertainty for the temperature difference in the thermal power formula can be

estimated in a much easier way. At typical operating conditions one has a temperature difference of about 25-30 K, with an average oil temperature of 200-230 °C, so that the uncertainty for a single temperature measurement is about $\sigma_T = 1.3\text{-}1.5$ °C (see above). Assuming uncorrelated inlet and outlet temperature measurements, one has $\sigma_{\Delta T} = \sqrt{(\sigma_{Tin}^2 + \sigma_{Tout}^2)} \approx \sqrt{2}\sigma_T = 1.8\text{-}2.1$ °C, yielding $\sigma_{\Delta T} / \Delta T = 6\text{-}8$ %. In transient phases, where $\Delta T = 5\text{-}10$ °C, much larger relative uncertainties can be reached (see section IV). It is evident that, for the considered system, this uncertainty source dominates with respect to the others, so that the thermal power uncertainty is approximately equal to this value. On the other hand, correlation between temperature measurements can be expected, so that this estimate can be considered as an upper bound for the actual uncertainty.

2) Thermal energy

Energy is given by the time integral of power. In practice, the integral has to be approximated by using the discrete available measurements. The simplest approximation is given by $E_{th} = \int P_{th}(t)\, dt \approx \Delta t \sum_i P_{th,i}$, where Δt is the acquisition time step, $P_{th,i}$ is the thermal power at the i-th step, and summation extends over N terms. Assuming uncorrelated quantities of the same order of magnitude (as, e.g., for stationary operation), after N measurements, a relative uncertainty reduction effect similar to the $1/\sqrt{N}$ factor for the average of repeated measurements would occur (see appendix).

However, as the nominal sensor uncertainty also covers possible bias errors, non-negligible correlations are expected. As mentioned for temperature sensors, in this context systematic errors could even dominate over random errors. Hence, in the absence of a more informed error model, we apply here the most conservative choice, assuming uncertainties to be mainly due to systematic errors and thereby fully correlated. As explained in the appendix, this yields the following formula for the relative energy uncertainty

$$\sigma_{Eth} / E_{th} = <\sigma_{Pth,i}> / <P_{th,i}>, \qquad (5)$$

where angle brackets represent averages on available measurements. As a rough estimate, one then has $\sigma_{Eth} / E_{th} = <\sigma_{Pth,i}> / <P_{th,i}> \approx \sigma_{Pth} / P_{th} \approx \sigma_{\Delta T} / \Delta T = 6\text{-}8$ % for the typical conditions considered above..

IV. APPLICATION TO THERMAL POWER AND LOSSES

As an example, in the following we show the application of uncertainty analysis to the estimation of output thermal power and of thermal losses in pipes.

A. Output thermal power

The total output thermal power of the HTF field is measured in the proximity of the heat exchanger connected to the steam generator. The considered sensors are the sensors $T_{HTF,IN}$, $T_{HTF,OUT}$, and M_{HTF} of Fig. 2. During the day, the output power increases and decreases according to the available solar radiation. The measured data for a summer day with good irradiance conditions are shown in Fig. 3. In the central part of the day, larger fluctuations are visible. These are due to a modulating behavior of the plant for large solar inputs: the flow rate is increased in order to limit temperatures and

hence pressures in the steam generator, which works with a pulsed operation. It is interesting to compare the observed fluctuations with the estimated power uncertainty. For the considered day, around noon one has $T_{ave} = 230$ °C and $\Delta T = 25$ °C, so that $\sigma_{\Delta T} / \Delta T = 8$ % and roughly the same holds for output power, while fluctuations are of the order of 20-25 %.

The figure clearly shows the variation of the power uncertainty along the day. Note that, while the absolute value is higher around noon, the relative value is higher in the morning and in the afternoon (reaching 35 % at 17:00). This is mainly due to the lower temperature differences in these cases.

The output thermal energy for the period shown in Fig. 3 is 1.9 MWh. The associated relative uncertainty, estimated according to (5), is about 9 % (i.e., 0.17 MWh of uncertainty).

B. Thermal losses

Here, only the connection pipes between the collector loops and the heat exchanger are considered. Estimating thermal losses on the basis of available parameters (insulation thermal conductivity, pipe geometric data, operating conditions), one gets an order of magnitude of 27 kW. With good irradiation conditions, the field output power is of the order of 350 kW, so that the above theoretical estimate yields thermal losses of about 8 % in full operation.

Experimentally, thermal losses are measured by calculating the difference between the output power of single collector loops and the output power measured at the heat exchanger, see Fig. 2. In Fig. 4 we show some real data plotted as a function of the difference between the oil temperature and the ambient temperature. Single points in the figure correspond to measured values averaged on a period of 20 min. Thermal losses clearly increase when this difference is larger. Besides single points, the figure shows their average within consecutive temperature intervals (bins) of 10 °C. The associated bars are calculated by propagating power uncertainties and clearly depend on operating conditions. It is also evident that these bars are larger than the statistical spreading of points (mainly due to varying operating conditions during the day).

During the most stable operating conditions, the average thermal losses are of the order of 35 kW, a value 30 % higher than the theoretically estimated one, thereby yielding losses of the order of 10 % with respect to the total output. On the other hand, the relative uncertainty is here of the order of 80 %.

V. CONCLUSIONS AND OUTLOOK

The measurement uncertainty presented above makes clear that the cost-effective sensors adopted for this monitoring system, while reasonably satisfactory for assessing the energy output of the solar field, fall short in guaranteeing an accurate analysis of the detailed aspects affecting performances.

In general, the sensors accuracy has of course to be tailored on the measurement purposes. From this point of view, a few cases of interest can be distinguished. A first case is related to the measurement of the thermal energy output. Then, one could compare the monitoring system with standard classes of heat meters. The standard EN 1434-1:2007 [16] considers three
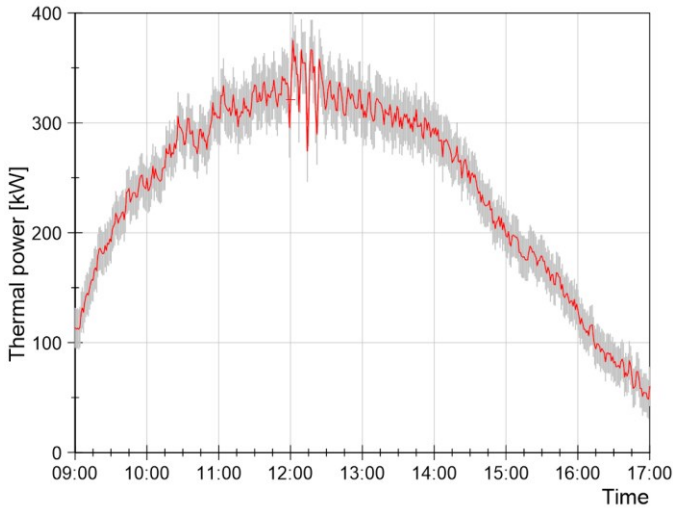
Fig. 3. Thermal output power of the HTF field for a typical summer day (July 2014). Central (red) curve: actual measured power (1 min sampling time.). Grey area around the central curve: estimated uncertainty.
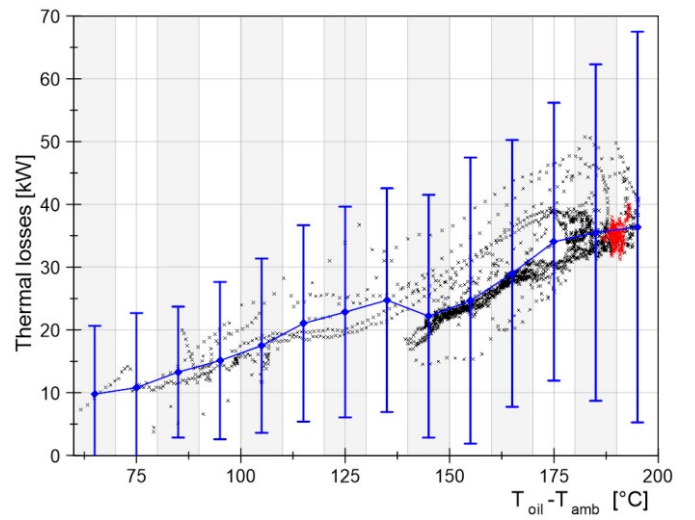

Fig. 4. Thermal losses in main pipes as a function of the difference between the average oil temperature and the ambient temperature. Black points: actual measurements taken during one week in July 2014, averaged on periods of 20 min. Red points (right): measurements taken only in relatively stationary conditions, when the system works at full power. Blue points: averages within temperature intervals of 10 °C; blue bars: propagated uncertainties.

classes: the maximum permissible relative error never exceeds 5 %. A second case, with slightly more demanding accuracy requirements, would be the detailed analysis of system operation. We have seen in Fig. 3 as the system fluctuations are of the order of 20-25 % in power. In order to follow this behavior with a relative uncertainty of 10 %, a relative measurement uncertainty of 2.5 % in output power would be needed. Finally, a third and even more restricting case would be given by a detailed analysis of thermal losses, which are of the order of 10 % with respect to the output power. In order to estimate them with a relative uncertainty of 10 %, a 1 % relative uncertainty in output power would be needed.

Among the mentioned cases, the most relevant one is certainly the thermal energy measurement. Although a standard uncertainty level ranging between 8 to 10 % is often acceptable from the industrial point of view, in order to reach a target of 5 %, one can act on the bottleneck given by temperature sensors. The simple substitution of class B Pt100 with class A Pt100, would basically cut the uncertainty in the temperature difference – and thereby in the output power and energy – by 50 %, basically reaching the target. A further lowering of the uncertainty would require to consider also other sensors, as under this threshold the uncertainty in the temperature difference would not dominate completely.

VI. APPENDIX

This appendix contains the technical details needed to carry out the calculations described in the text.

A. Thermal oil properties

The diathermic oil used at the Soltigua field is Therminol SP, produced by Solutia. The data sheet provides experimental data for the main fluid properties as a function of temperature, as well as analytic formulas for their calculation. The dependence of density and specific heat on temperature (expressed in °C) is well approximated by the following

equations (relative error with respect to experimental data: < 0.1 % for ρ and < 0.025 % for C_p in the interval 0-250 °C):

$$\rho(T) \ [kg/m^3] = 885.597 - 0.689367 \cdot T + 1.9228 \cdot 10^{-4} \cdot T^2 + \\ - 8.87642 \cdot 10^{-7} \cdot T^3$$

$$C_p(T) \ [J/(kg \cdot K)] = 1833.69 + 3.6172 \cdot T - 4.94238 \cdot 10^{-4} \cdot T^2 + \\ + 7.98115 \cdot 10^{-7} \cdot T^3$$

When propagating uncertainties, one has to take into account derivatives with respect to temperature. Simple calculations show that in the interesting ranges one has

$$\sigma_\rho/\rho = |(T/\rho) \ (d\rho/dT)| \ (\sigma_T/T) \le 0.05\text{-}0.3 \ \sigma_T/T \ ,$$

$$\sigma_{Cp}/C_p = |(T/C_p) \ (dC_p/dT)| \ (\sigma_T/T) \le 0.3 \ \sigma_T/T \ .$$

Properly combining with the relative temperature uncertainty σ_T/T in the different cases, one gets the relative uncertainty reported in the text, which can be safely neglected with respect to other error sources.

B. Uncertainty propagation in the presence of correlations

Below, we recall the effects of correlations in measurements [17]. For a function of multiple variables $f(x_1, \dots, x_N)$, the propagated uncertainty σ_f is

$$\sigma_f \quad = \sqrt{[\Sigma_{i,j} \ (\partial f/\partial x_i) \ (\partial f/\partial x_j) \ V_{ij}]} = \\ = \sqrt{[\ \Sigma_i \ (\partial f/\partial x_i)^2 \ \sigma_{xi}^2 + 2\Sigma_{i<j} \ (\partial f/\partial x_i) \ (\partial f/\partial x_j) \ V_{ij}]} \ ,$$

where $V_{ij} = \langle(x_i - \langle x_i\rangle)(x_j - \langle x_j\rangle)\rangle$ is the covariance matrix (angle brackets represent expected values; in the case of repeated measurements they can be estimated as averages) and $\sigma_{xi}^2 = V_{ii}$. For uncorrelated variables one has $V_{ij} = 0$ for $i \ne j$ and the formula reduces to the usual root mean square calculation.

In the case of energy measurements, correlations can appear in the presence of systematic errors. As mentioned in

the body of the paper, thermal energy can be expressed as $E = \Delta t \sum_i P_i$, with $i = 1, \ldots, N$ (in this appendix we drop the "th" subscript for brevity). With respect to the above discussion, the role of the variables x_i is here played by the power measurements P_i. For simplicity, we assume here that all the power measurements are of the same order, $P_i = P$ (stationary operation) and that each power measurement has the same uncertainty, $\sigma_{Pi} = \sigma_P$. Then, if all the measurements were uncorrelated ($V_{ij} = 0$ for $i \neq j$), the relative uncertainty for the energy would decrease with the number of measurements similarly to the uncertainty of a statistical average:

$$\sigma_E / E = \sqrt{[\sum_i (\Delta t)^2 \, \sigma_P^2]} / (\Delta t \sum_i P) = (\sigma_P / P) / \sqrt{N} .$$

However, this would not hold in the presence of correlations. For example, if the uncertainty σ_P on the power measurements could be mainly attributed to a constant offset (i.e., a systematic error), then one would have the limiting case of fully correlated measurements, where $V_{ij} = V_{ii} = \sigma_P^2$. The relative energy uncertainty would then be equal to the relative power uncertainty, without any decrease:

$$\sigma_E / E = \sqrt{[\sum_i (\Delta t)^2 \, \sigma_P^2 + 2\sum_{i<j} (\Delta t)^2 \, \sigma_P^2]} / (\Delta t \sum_i P) =$$
$$= (\sigma_P / P) \sqrt{[N + N(N-1)]} / N = \sigma_P / P .$$

It is of course very difficult to assess the actual amount of systematic errors in energy measurements. Clearly, the assumption of uncorrelated power measurements would be too optimistic, leading to a vanishing relative uncertainty for long acquisition campaigns. Moreover, real systems are typically non-stationary, so that different uncertainties should be taken into account depending on the operating conditions. The most conservative choice (adopted here) is to assume that the power uncertainty is mainly due to constant systematic effects. This would correspond to the situation where $V_{ij} = \sigma_{xi}\sigma_{xj}$ (perfectly correlated measurements with variable uncertainties). Then

$$\sigma_f = \sqrt{[\sum_i (\partial f/\partial x_i)^2 \, \sigma_{xi}^2 + 2\sum_{i<j} (\partial f/\partial x_i) (\partial f/\partial x_j) \, \sigma_{xi}\sigma_{xj}]} =$$
$$= \sqrt{[\sum_{i,j} (\partial f/\partial x_i) (\partial f/\partial x_j) \, \sigma_{xi}\sigma_{xj}]} = \sum_i (\partial f/\partial x_i) \, \sigma_{xi} ,$$

i.e., one has a linear sum instead of a square root sum. Equation (5) is obtained by applying this formula to the relative energy uncertainty.

REFERENCES

[1] S. Kalogirou, "The potential of solar industrial process heat applications", Applied Energy, vol. 76, pp. 337-361 (2003).

[2] C. Lauterbach, B. Schmitt, U. Jordan, and K. Vajen, "The potential of solar heat for industrial processes in Germany", Renewable and Sustainable Energy Reviews, vol. 16, pp. 5121-5130 (2012).

[3] A. Vittoriosi et al., "Monitoring of a MW class solar field set up in a bricj manufacturing process", Energy Procedia, vol. 48, pp. 1217-1225 (2014).

[4] A. Giostri, M. Binotti, P. Silva, E. Macchi, and G. Manzolini, "Comparison of two linear collectors in solar thermal plants: parabolic trough versus Fresnel", Journal of Solar Energy Engineering, vol. 135, pp. 011001-(1-9) (2013).

[5] G. Morin, J. Dersch, W. Platzer, M. Eck, and A. Haberle, "Comparison of Linear Fresnel and Parabolic Trough Collector Power Plants," Sol. Energy, vol. 86, pp. 1-12 (2012).

[6] N. El Gharbi, H. Derbal, S. Bouaichaoui, N. Said, "A comparative study between parabolic trough collector and linear Fresnel reflector technologies", Energy Procedia, vol. 6, pp. 565-572 (2011).

[7] D. R. Mills, P. Le Lievre, G. L. Morrison, "First results from compact linear Fresnel reflector installation". In: Proceedings of ANZSES Solar2004 (2004).

[8] R. Gabbrielli, P. Castrataro, F. Del Medico, M. Di Palo, B. Lenzo, "Levelized cost of heat for linear Fresnel concentrated solar systems", Energy Procedia, vol. 49, pp. 1340-1349 (2014).

[9] EN 12975:2006, Thermal Solar Systems and Components – Solar Collectors – Part 1: general requirements, Part 2: Test Methods (2006).

[10] S. Fischer, E. Lüpfert, H. Müller-Steinhagen, "Efficiency testing of parabolic trough collectors using the quasi-dynamic test procedure according to the european standard EN 12975". In: Proceedings of 13th SolarPACES conference (2006).

[11] S. Fischer, H. Drück, "Standards and certification schemes for solar thermal collectors, stores and systems - An overview about the latest developments", Energy Procedia, vol. 57, pp. 2867-2871 (2014). In: Proceedings of the 2013 ISES Solar World Congress.

[12] EN ISO 9806:2013, Solar energy – Solar thermal collectors – Test methods (2013).

[13] F. Sallaberry, R. Pujol-Nadal, A. Garcia de Jalón, V. Martínez-Moll, "Towards a standard testing methodology for medium temperature solar collectors with variable geometry", Energy Procedia, vol. 57, pp. 2904-2913 (2014). In: Proceedings of the 2013 ISES Solar World Congress.

[14] ASME MFC 14M, Measurement of Fluid Flow Using Small Bore Precision Orifice Meters (2003).

[15] ISO 5167-2:2003, Measurement of fluid flow by means of pressure differential devices inserted in circular cross-section conduits running full – Part 2: Orifice plates (2003).

[16] EN 1434-1:2007, Heat meters – Part 1: General requirements (2007).

[17] ISO/IEC Guide 98-3:2008, Uncertainty of measurement – Part 3: Guide to the expression of uncertainty in measurement (2008).